Studies on a High-Temperature Regenerative Heat Exchanger for Closed-Cycle MHD Power Generation

Yoon-Sik Kim *

Yuuichi Shinagawa, Kunio Yoshikawa and Susumu Shioda **

A numerical heat-transfer analysis in the combustion chamber of a pebble bed regenerative heat exchanger has been carried out for the heating period. A radiative zone method coupled with chemical and two-dimensional fluid dynamic calculations is employed in the analysis, and the results agree well with the measured data. The analysis also shows that higher temperature can be obtained at the top of the pebble bed by optimizing the geometries of the combustion chamber and the burner.

1. Introduction

In a closed-cycle MHD power generation system, regenerative heat exchangers are used for heating the working inert gas(argon or helium) to about 1650℃, while the impurity level in the working gas is kept below 100 ppm.

In the heat exchanger concerned with here, the combustion gas and the inert gas pass through the same heat storage bed alternately. Thus multiple heat exchangers are required to supply a continuous flow of high temperature inert gas to an MHD generator.

To suppress any mixing of the combustion and inert gases, each heat exchanger will be cyclically operated in four operational periods : (1) heating the heat storage bed by the combustion gas, (2) evacuation of the residual combustion gas inside the heat exchanger, (3) heating the inert gas by the heat storage bed, and (4) recovery of the residual inert gas inside the heat exchanger.

Therefore the heat-transfer processes inside the heat exchanger are inherently unsteady, which requires an unsteady heat-transfer analysis for optimum designing of the heat exchanger.

A regenerative heat exchanger consists of a combustion chamber and a heat storage bed. An unsteady heat-transfer analysis regarding the heat storage bed(pebble bed) has previously been reported in [1]. An unsteady heat-transfer analysis in the combustion chamber for each operational period should also be performed to simulate the complete thermal performance of such a heat exchanger. For the combustion gas heating period, it is essential to heat the top of the bed up to a temperature as high as possible to maximize the temperature of the inert gas at exit of the heat exchanger.

In this paper, a heat-transfer analysis in the combustion chamber is performed for the combustion gas

* Department of Marine Engine, Korea Maritime University

** Department of Energy Sciences, Tokyo Institute of Technology

heating period. The combustion gas temperature in the combustion chamber is so high (well above 1800 ℃) that the analysis is focused on the radiative heat transfer, and this heat-transfer analysis is combined with the fluid dynamical analysis to simulate the flow and temperature fields in the combustion chamber during the combustion of natural gas. Then using a numerical analysis, the optimum geometries for the combustion chamber as well as for the burner are determined to maximize the temperature at the top of the bed during the combustion gas heating period.

The structure of the combustion chamber in the pebble bed regenerative heat exchanged used for the experiments is shown in Fig. 1. This heat exchanger is for high temperature argon heating. The total height of the combustion chamber is 2.3m, and a burner is installed at the central uppermost portion of it. The diameter of the chamber is 1.1m and it is surrounded by a four-layered insulating wall(whose thickness is 0.25m).

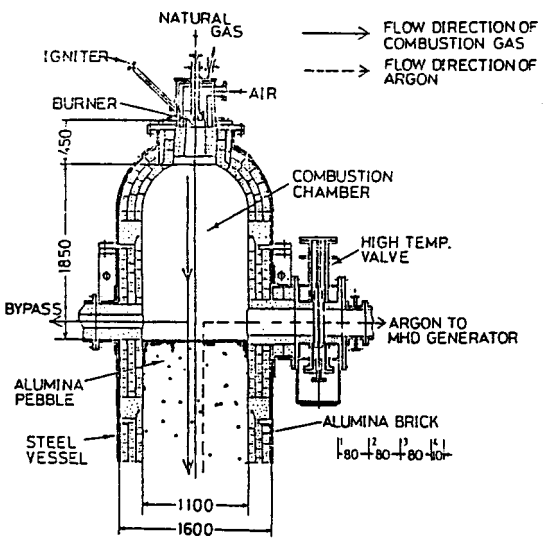

Fig. 1 Structure of the combution chamber in the pebble bed regenerative heat exchanger.

Natural gas is supplied to the combustion chamber through a fuel nozzle located at the center of the burner, and it is burned with preheated air (250℃) supplied through tapered air nozzles located around the fuel nozzle. The combustion gas passes through the pebble bed for about 30 hours (the heating period), and the top of the pebble bed is heated up to about 1850℃ at the end of this period.

In the present numerical analysis, the steady temperature distribution and flow field in the combustion chamber at the end of this heating period are obtained.

2. Basic Equations and Numerical Method

The flow field can be described by the following two-dimensional steady elliptic differential equation in terms of the dependent variable ψ in an axisymmetric cylindrical coordinate system [2].

$$a\left[\frac{\partial}{\partial z}\left(\phi\frac{\partial\psi}{\partial r}\right)-\frac{\partial}{\partial r}\left(\phi\frac{\partial\psi}{\partial z}\right)\right]-\frac{\partial}{\partial z}\left[b\frac{\partial}{\partial r}(c\phi)\right]-\frac{\partial}{\partial r}\left[b\frac{\partial}{\partial r}(c\phi)\right]+d=0 \qquad (1)$$

Table 1 shows each dependent variable and its related coefficients. The dependent variables to be solved are the stream function ψ, the vorticity ω/r, the swirl velocity rV_θ, the fuel mass fraction m_f, the air mass fraction m_0, and the enthalpy i. Since the main heat-transfer process is considered to be radiation rather than convection, a simple turbulence model [2] is employed in the present analysis, which is

$$\mu t = \kappa D^{2/3} L^{-1/3} \rho^{2/3} (\dot{m}_f U_f^2 + \dot{m}_0 U_0^2)^{1/3} \tag{2}$$

The turbulent diffusion coefficients which appear in the mass fraction equations and the enthalpy are defined as follows :

$$\Gamma_{jt} = \frac{\mu_t}{\sigma_{jt}} \tag{3}$$

$$\Gamma_{it} = \frac{\mu_t}{\sigma_{it}} \tag{4}$$

where the subscript j represents fuel f or air 0, and both the turbulent Schmidt number Γ_{jt} and the turbulent Prandtl number Γ_{it} assumed to be 1.0

The boundary conditions for each dependent variable are summarized in Table 2. The boundary conditions for the enthalpy i at the insulating wall and at the exit(i.e., at the top of the pebble bed), which

Table 1 Dependent Variables and Their Coefficients

	φ	a	b	c	d
1.	ω	r^2	r^3	μt	$\bar{d}$
2.	Ψ	0	$\frac{1}{\rho r}$	1	$-\omega$
3.	rV_θ	1	$\mu_t r^3$	$\frac{1}{r^2}$	0
4.	m_f	1	$\Gamma_{ft}\, r$	1	$-rS_f$
5.	m_o	1	$\Gamma_{ot}\, r$	1	$-rS_o$
6.	i	1	$\Gamma_{it}\, r$	1	rS_i

$$\bar{d} = -r\frac{\partial}{\partial z}(\rho v_\theta^2) - r^2\left\{\frac{\partial}{\partial z}\left(\frac{u^2+v^2}{2}\right)\frac{\partial \rho}{\partial r} - \frac{\partial}{\partial r}\left(\frac{u^2+v^2}{2}\right)\frac{\partial \rho}{\partial z}\right\}$$

Table 2 Boundary Conditions

ϕ	ω/r	ψ	rVθ	m	i
Inlet	$\phi = \phi_{in}$				
Wall	$\phi = \phi_{wb}$	0		$\partial\phi/\partial r, z = 0$	*
Axis of symmetry	0	$\phi = \phi_c$	0	$\partial\phi/\partial r = 0$	
Exit	$\partial\phi/\partial z = 0$				*

are indicated by * in Table 2, are given by

$$h_w A_{gw}(T_w - T_0) + A_{gw}\varepsilon_w \sigma T_w^4 = h_{gw} A_{gw}(T_g - T_w) + Q_{rin} \tag{5}$$

$$k_{pz} A_p \frac{dT_p}{dz} + A_p \varepsilon_p \sigma T_p^4 = h_{gp} A_{gp}(T_g - T_p)\, Q_{rin} \tag{6}$$

In Eq. (5), the first and second terms on the left-hand side represent the heat conduction through the insulating wall and the radiative heat emission, respectively. The first and second terms on the right-hand side represent the convective heat transfer between the gas and the wall, and the radiative heat flux from other wall or gas zones, respectively.

Equation (6) is a similar relation for the top of the pebble bed. In Eq. (5), the effective thermal conductivity for the h_w four-layered insulating wall is given by

$$h_w = \frac{1}{\left[r_0 \sum_{m=1}^{4} \frac{(r_{mo}/r_{mi})}{k_{wm}}\right]} \tag{7}$$

The convective heat-transfer coefficient h_{gw} between the combustion gas and the insulating wall was evaluated by the following equation [3] :

$$N_u = 0.023\, Re^{0.8}\, Pr^{1/3} \tag{8}$$

In Eq. (6), the effective axial thermal conductivity in the pebble bed k_{pz} was evaluated by the equation given in [4], and the heat-transfer coefficient h_{gp} between the conbustion gas and pebbles was evaluated by [5].

$$h_{gp} = \frac{0.255}{\alpha} Pr^{1/3}\, Re^{2/3}\, \frac{k_g}{d_p} \tag{9}$$

The chemical reaction associated with the combustion process of natural gas is assumed to be a single-step chemical reaction whose reaction rate is given by the following Arrhenius expression [6] :

$$R_c = A_c e^{-Ea/RT} [m_f]^a [m_o]^b \tag{10}$$

Conditions for the calculation and the coefficients which appear in Eq. (10) are summarized in Table 3. The grid configuration in the calculation is shown in Fig. 2. Here, the hemispherical shape of the dome section is approximated by a cylinder. The right-half side shows the grid spacing for the flow field calculation and the left-half side shows the zone division (configuration) for the radiation calculation described below.

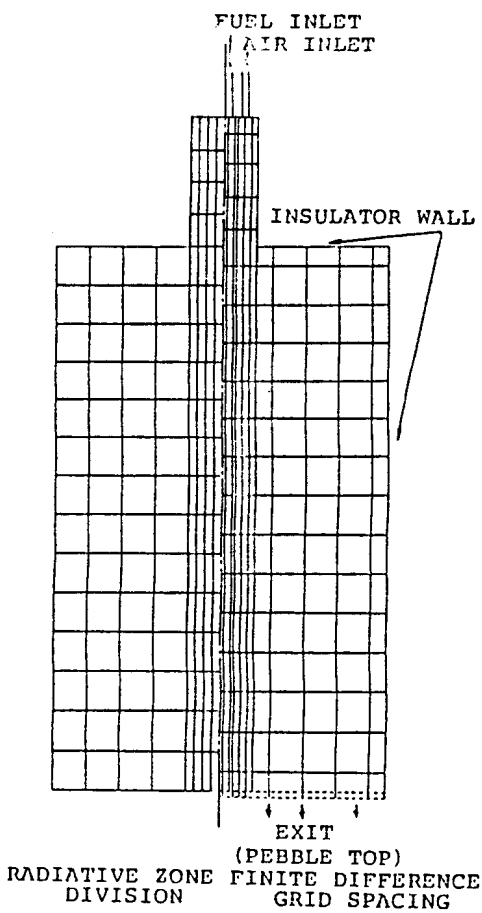

Fig. 2 Grid configuration in the calculation.

Table 3 Coefficients Used and Conditions Assumed

Conditions for Combustion	
Fuel mass flow rate	: 0.014 kg/s
Air mass flow rate	: 0.236 kg/s
Inlet air temperature	: 250 ℃
Inlet fuel temperature	: 25 ℃
Insulator outer wall temperature	: 230 ℃
Combustion gas pressure	: 0.13 Mpa
Constants Used	
Coefficient for turbulent viscosity	κ : 0.012
Collision frequency factor	A_c : 2.8×10^9
Activation energy (Kcal / mol)	E_a : 48.4
Constant for chemical reaction	a : −0.3
Constant for chemical reaction	b : 1.3

3. Modeling for the Radiative Heat Transfer

In the enthalpy equation for the heating period, the source term S_i can be expressed as

$$S_i = R_c \Delta H_c + S_r \tag{11}$$

where the first and the second terms on the right-hand side represent the generation of heat by combustion and the net enthalpy change by the radiative heat transfer, respectively.

The combustion chamber is divided into gas zones and wall zones in order to apply the zone method proposed by Hottel et al. [7].

The radiative heat-transfer term, Sr for the gas zone k, whose volume is V_k, can be expressed as

$$S_r V_k = -4\sum_{n=1}^{3} a'n(T_k)k_n V_k \sigma T_k^4 + 4\sum_{n=1}^{3}\sum_{j} a'_n(T_j)k_n V_j (f_{jk})_n \sigma T_j^4 + \sum_{n=1}^{3}\sum_{i} a_n(T_i)A_i \varepsilon_i (f_{ik})_n \sigma T_i^4 \tag{12}$$

The first, second, and third terms on the right-hand side are the radiative emission from the zone V_k, the amount of radiation received from all gas zones V_j and the amount of radiation received from all wall zones A_i. The combustion gas was represented by a mixture of three gray gases and a clear gas with different absorption coefficient k_n [7], and a_n' and a_n are weighting factors for the emissivity and the absorptivity, respectively. In Eq. (12), $(f_{ij})_n$ is the geometry dependent radiative exchange factor for each gray gas and it was calculated by the Monte Carlo method [8, 9].

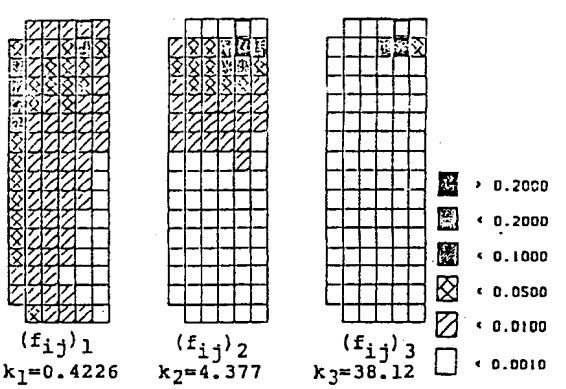

Fig. 3 Distribution of $(Fij)_n$ for the three gray gases with different absorption coefficient.

Figure 3 shows the distribution of f_{ij} for the three gray gases with different absorption coefficients, where a number of radiative particles are emitted from the upper wall zone enclosed by the bold rectangle. As the absorption coefficient becomes smaller, the radiative energy is shown to spread more evenly in the combustion chamber.

4. Results and Discussion

4.1 Effects of the emissivity of the insulating wall

In the simulation model described above, the emissivities for the insulation wall ε_w and for the top of the pebble bed ε_p have not yet been defined. These parameters depend not only on temperature but also on the material and the surface condition. There are no accurate values for ε_w available as a function of temperature, but those for ε_p were measured by comparing the temperature data at the top of the pebble

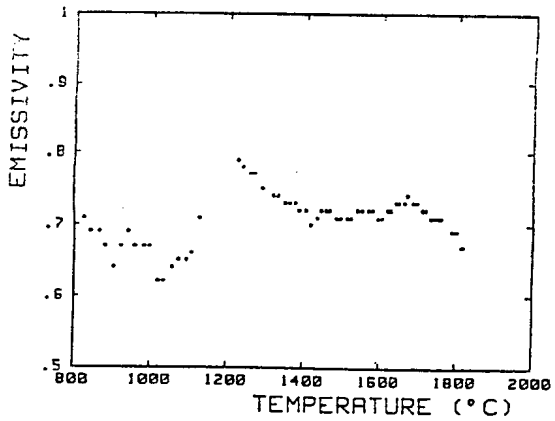

Fig. 4 Measured emissivity of the top of the pebble bed as a function of temperature.

bed obtained from a pyrometer and a thermocouple. The results are shown in Fig. 4. Which indicates that ε_p has values between 0.7 and 0.8 in the temperature range of 1400~1800℃. Therefore, in this simulation, ε_p was assumed to have a constant value of 0.75, and because the insulating wall and pebbles are made from the same material (alumina), ε_w was assumed to be equal to ε_p.

Figure 5 shows the distribution of the stream function normalized by the value at the inlet of the combustion chamber, which indicates a large recirculating flow.

Figure 6 shows the temperature distribution in the combustion chamber. The highest temperature zone is located near the center of the combustion chamber, and some temperature drop is observed toward the top of the pebble bed.

Figure 7 shows how the combustion gas temperature distribution in the combustion chamber changes

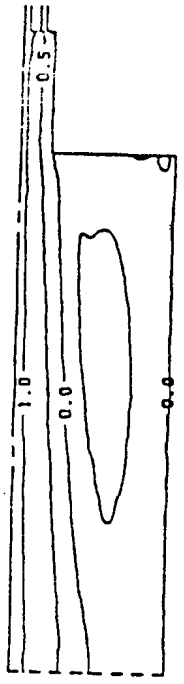

Fig. 5 Flow pattern of combustion gas in the combustion chamber.

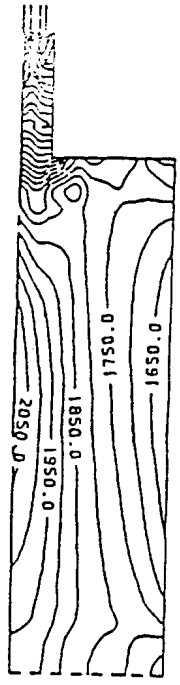

Fig. 6 Temperature distribution in the combustion chamber.

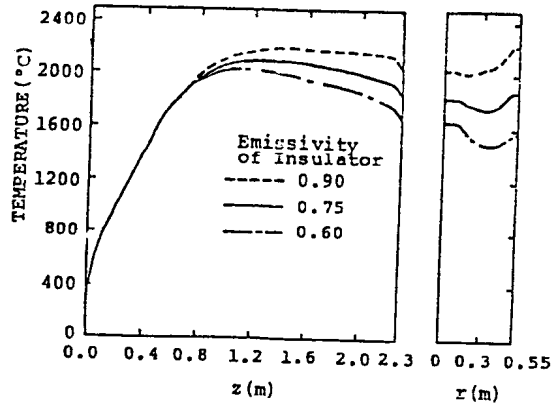

Fig. 7 Axial temperature profile in the combustion chamber and radial temperature profile at the top of the pebble bed for combustion gas.

when ε_w varies. The left-hand figure shows the axial temperature distribution and the right-hand figure shows the radial distribution at the top of the pebble bed. The experimentally measured temperature at the top of the pebble bed is about 1850℃, which agrees with the simulation result when ε_w is 0.75. When ε_w is taken as 0.90 or 0.60, the simulated temperature at the top of the pebble bed differs from that for the case of ε_w = 0.75 by more than 200℃. This means that radiation is the major mechanism for the heat-transfer processes in the combustion chamber.

4.2 Effects of the convective heat transfer

In order to clarify the importance of the convective heat transfer between the combustion gas and the insulating wall, the same calculation was performed by taking the convective heat-transfer coefficient h_{gw} as 0. The results obtained were almost the same as those shown in Fig. 7, and the small temperature drop at the top of the pebble bed as a result of neglecting the convective heat transfer is about 20℃. This indicates that convection has only a minor effect on the heattransfer processes and the evaluation of h_{gw} is not a critical problem.

4.3 Effects of the geometries of the combustion chamber and the burner

From the standpoint of an MHD generator, the heated argon temperature and thus that of the pebbles at the top of the bed should be maximized for a fixed burner capacity. Therefore the effects of the combustion chamber geometry and the burner geometry on the obtainable pebble temperature at the top of the bed were investigated by the use of the above simulation code.

Figure 8 shows the pebble temperature in the center of the top of the bed as functions of the height and the diameter of the combustion chamber. This figure indicates that a higher pebble temperature is obtainable by reducing the height and the diameter, unless the height is too low for completing the combustion within the combustion chamber. Since the minimum combustion chamber diameter, which is the same as that of the pebble bed, is determined mainly by the allowable argon pressure loss through the pebble bed, the optimization of the height of the combustion chamber is a main concern. Figure 8 suggests that the top of the bed can be heated up to an even higher temperature by reducing the height from the present value(= 2.3 m)

Figure 9 illustrates the effect of the swirl ratio (azimuthal velocity/axial velocity) of the combustion air on the pebble temperature at the top of the bed, when the height and diameter of the combustion chamber is 2.3 m and 1.1 m, respectively.

When the radial distance between the fuel nozzle and the air nozzles is 0.066 m, which is the value for the present heat exchanger, that temperature decreases by increasing the swirl ratio. A high swirl ratio of combustion air promotes the mixing of fuel and air, which results in a shift of the highest flame temperature zone in the upstream direction, and the gas temperature at the top of the bed shows some

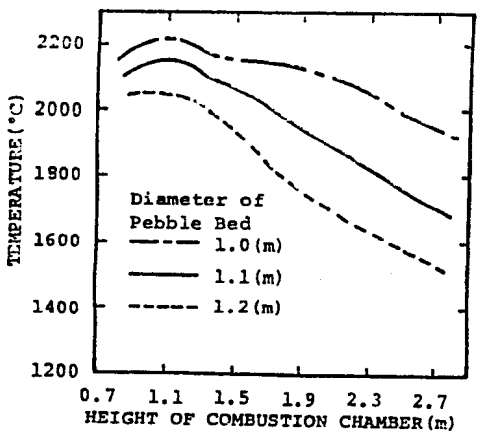

Fig. 8 Pebble temperature at the top of the bed as function of the height and diameter of combustion chamber.

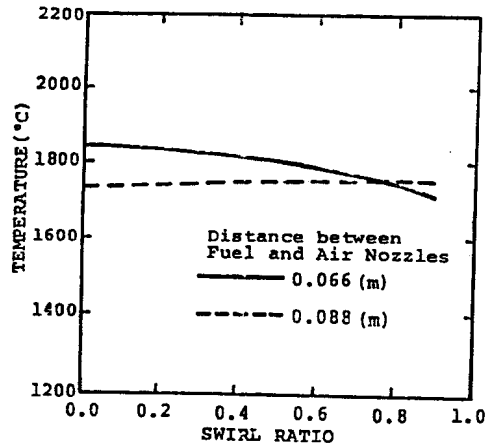

Fig. 9 Pebble temperature at the top of the bed as function of the swirl ratio of combustion air and the distance between fuel and air nozzles of the burner.

When the radial distance between the fuel and air nozzles is increased to 0.088m, a good mixing of fuel and air requires a higher swirl ratio. Thus an increase of the swirl ratio results in a higher pebble temperature at the top of the bed. These results indicate the importance of the burner geometry.

5. Conclusions

A two-dimensional heat-transfer and fluid-dynamics analysis in the combustion chamber of a pebble-bed regenerative heat exchanger has been performed for the combustion period. The zone method was employed in modeling the radiative heat transfer and the combustion reaction was represented by a single-step chemical reaction whose reaction rate is given by the Arrhenius equation. The calculation estimates satisfacorily the pebble temperature at the top of the bed measured during combustion. The simulation also shows that geometry optimization is important both for the combustion chamber and for the burner to maximize the pebble temperature at the top of the bed for a fixed burner capacity.

Nomenclature

A_p : heat-transfer area per unit volume at the top of the pebble bed

A_{gp} : heat-transfer area between combustion gas and pebbles per unit volume

A_{gw} : heat-transfer area between combustion gas and insulating wall per unit volume

D : diameter of combustion chamber

d_p : diameter of pebbles

ΔH_c : calorific value of natural gas

h_{gp} : convective heat-transfer coefficient between combustion gas and pebbles

h_{gw} : convective heat-transfer coefficient between combustion gas and insulating wall.
k_g : thermal conductivity of combustion gas
k_{pz} : effective thermal conductivity in pebble bed
$\dot{m}$: mass flow rate of combustion gas per unit area of pebble bed
N_u : Nusselt number
P_r : Prandtl number
R_e : Reynolds number
r : radial coordinate
r_0 : radius of combustion chamber
T : temperature
T_0 : temperature of outer shell of heat exchanger
z : axial coordinate
α : void fraction of pebble bed
ε : emissivity
ρ : density
μt : turbulent viscosity
σ : Stefan-Boltzmann constant

Subscripts

f : fuel
g : combustion gas
o : air
p : pebble
ω : insulating wall

Literature Cited

1. K. Yoskikawa, S. Kabashima, and S. Shioda, *Heat Transf. Jpn. Res.*, 16, 78 (1987).
2. A.D. Gosman, W.M. Pun, A.K. Runchal, D.B. Spalding, and M.Wolfshtein. *Heat and Mass Transfer in Recirculating Flows*, Academic Press (1969).
3. *JSME Data Book : Heat Transfer* (3rd ed.), 28 (1975).
4. S. Yagi and D. Kunii. *Kagaku Kogaku*, 18, 576 (1954) (in Japanese).
5. A.G. Dixon and D.L. Gresswell. *AIChE J.*, 25, 663 (1979).
6. K.W. Charles and L.D. Fredrick. *Prog. Energy Com. Sci.*, 10, 1 (1984).
7. H.C. Hottel and A.F. Sarofim. *Int. J. Heat Mass Transf.*, 8, 1153 (1965).
8. J.R. Howell and M. Perlmutter. *Trans. ASME. J. Heat Transf.*, 86, 116 (1964).
9. M. Perlmutter and J.R. Howell. *Trans. ASME. J. Heat Transf.*, 86, 169 (1964).